



Published in final edited form as:

Inflamm Bowel Dis. 2011 May ; 17(5): 1163–1176. doi:10.1002/ibd.21469.

Nanoparticle-based therapeutic delivery of prohibitin to the colonic epithelial cells ameliorates acute murine colitis

Arianne L. Theiss, Ph.D.^{1,*}, Hamed Laroui, Ph.D.¹, Tracy S. Obertone, Ph.D.¹, Indrajit Chowdhury, Ph.D.², Winston E. Thompson, Ph.D.², Didier Merlin, Ph.D.¹, and Shanthi V. Sitaraman, M.D., Ph.D.¹

¹Division of Digestive Diseases, Department of Medicine, Emory University, Atlanta, GA 30322

²Department of Obstetrics and Gynecology, Morehouse School of Medicine, Atlanta, GA 30310

Abstract

Introduction—Intestinal epithelial expression of anti-oxidants and NF- κ B contribute to mucosal barrier integrity and epithelial homeostasis, two key events in the pathogenesis of inflammatory bowel disease. Genetic restoration of intestinal epithelial prohibitin 1 (PHB) levels during experimental colitis reduces the severity of disease through sustained epithelial anti-oxidant expression and reduced NF- κ B activation. To determine the therapeutic potential of restoring epithelial PHB during experimental colitis in mice, we assessed two methods of PHB colonic mucosal delivery: adenovirus-directed administration by enema and poly (lactic acid) nanoparticle (NPs) delivery by gavage.

Methods—As a proof-of-principle to demonstrate the therapeutic efficacy of PHB, we utilized adenovirus-directed administration by enema. Second, we used NPs based colonic delivery of biologically active PHB to demonstrate therapeutic use for human IBD. Colitis was induced by oral administration of dextran sodium sulfate in water for 6–7 days. Wild-type mice receiving normal tap water served as controls.

Results—Both methods of delivery resulted in increased levels of PHB in the surface epithelial cells of the colon and reduced severity of dextran sodium sulfate-induced colitis in mice as measured by body weight loss, clinical score, myeloperoxidase activity, pro-inflammatory cytokine expression, histological score and protein carbonyl content.

Conclusions—This is the first study to show oral delivery of a biologically active protein by NPs encapsulated in hydrogel to the colon. Here we show that therapeutic delivery of PHB to the colon reduces the severity of dextran sodium sulfate-induced colitis in mice. PHB may represent a novel therapeutic target in inflammatory bowel disease.

Keywords

animal models of IBD; nanotechnology; gene therapy; colitis

*Address correspondence to: Arianne L. Theiss, Division of Digestive Diseases, 615 Michael Street, Whitehead Biomedical Research Building 265, Atlanta, Georgia 30322, Tel: 404-712-2862, Fax: 404-727-5767, atheiss@emory.edu.

Conflicts of Interest: The authors disclose no conflicts.

Author Contributions:

Conceived and designed the experiments: ALT, HL, DM, SVS. Performed the experiments: ALT, HL, TSO, IC. Analyzed the data: ALT, HL, SVS. Contributed reagents/materials/analysis tools: ALT, IC, WET, DM, SVS. Wrote the paper: ALT, SVS.

Competing Financial Interests:

No competing financial interests exist for any author.

Introduction

Although the etiologies of the two major forms of inflammatory bowel disease (IBD), Crohn's disease and ulcerative colitis, remain unknown, evidence suggests that in addition to the widely accepted aberrant mucosal immune response, non-immune cells including epithelial cells play an emerging role in the pathogenesis of disease.¹ Multiple epithelial molecules have been identified as mediators of IBD pathogenesis including those that control mucosal barrier integrity and epithelial homeostasis.

Intestinal epithelial NF- κ B plays a central role in the pathogenesis of IBD and current evidence suggests that levels of epithelial NF- κ B must be held in balance; increased expression of NF- κ B, as occurs in IBD inflamed colonic mucosal biopsies, not only contributes to the pathogenesis of disease by altering intestinal barrier function² but also activates proinflammatory signaling³ thereby promoting the inflammatory process, whereas complete ablation of intestinal epithelial p65 expression in mice resulted in deregulated response to injury and inflammation and decreased animal survival.⁴ Therefore, molecules that can inhibit but not completely abolish expression of NF- κ B may make optimal therapeutic targets for IBD.

Prohibitin 1 (PHB) is an evolutionarily conserved, multifunctional 30 kDa protein implicated in cellular processes including mitochondrial function and protein folding,^{5, 6} proliferation control and suppression of oncogenesis,^{7, 8} and transcriptional regulation.⁹⁻¹¹ Expression of PHB is decreased in mucosal biopsies from ulcerative colitis and Crohn's disease afflicted patients and in animal models of colitis.^{12, 13} Pro-inflammatory cytokines such as tumor necrosis factor alpha (TNF α) decrease expression of intestinal epithelial PHB in vivo and in vitro.¹⁴ Our recent data suggest that epithelial PHB sustains anti-oxidant expression and has anti-inflammatory properties. Restoration of PHB levels in intestinal epithelial cells during colitis using transgenic mice overexpressing PHB under the control of the intestinal epithelial-specific villin promoter reduced the severity of colitis by acting as a regulator of increased anti-oxidant response.¹⁵ Importantly, sustained expression of PHB in intestinal epithelial cells reduced TNF α -stimulated NF- κ B activation in vivo and in vitro through a novel mechanism of inhibition of p65 nuclear translocation involving alteration of importin α 3 levels.¹⁴

To determine the therapeutic potential of restoring epithelial PHB during experimental colitis in mice, we assessed two methods of PHB colonic mucosal delivery: adenovirus-directed administration by enema and nanoparticles (NPs) delivery by gavage. To our knowledge, this is the first study to show oral delivery of a biologically active protein by NPs encapsulated in a hydrogel to the colon. Here we show that therapeutic delivery of PHB to the colon reduces the severity of colitis in mice.

Materials and Methods

Generation of recombinant adenoviral vectors

The prohibitin gene (PHB1) was subcloned into the pAdTrack-cytomegalovirus-GFP vector to generate pAdTrack-CMV-PHB1-GFP (AdPHB) as previously described.¹⁶ Therefore, the resultant plasmid encoded the PHB1 gene under the control of a CMV promoter followed by the GFP gene. pAdTrack-CMV-GFP was used as a vector control (AdV).

Enema administration of recombinant adenovirus to mice

All procedures using mice were in accordance with Emory University Institutional Animal Care and Use Committee. Wild-type (WT), C57BL/6J male 8-week old mice were purchased from Jackson Laboratories (Bar Harbor, ME). Mice were anesthetized with

isoflurane (Baxter Healthcare, Deerfield, IL) and given an intrarectal enema of 100 μ l 50% ethanol (vol/vol) diluted in distilled H₂O using a catheter (Instech Solomon Scientific, Plymouth Meeting, PA) attached to a 1 ml syringe. The catheter was inserted 3 cm proximal to the anus. Mice were held in a vertical position for 30 s after the enema to prevent leakage from the anus. Mice were allowed 3 h to recover, anesthetized again, and given another enema of 50 μ l of phosphate-buffered saline (PBS) alone or PBS containing 2×10^9 adenoviral-vector (AdV) or AdPHB plaque-forming units (pfu). Mice were monitored and weighed daily.

To assess AdPHB infection, mice were sacrificed 1, 3 and 5 days post-infection. Colon was excised and processed for GFP localization by confocal microscopy or mucosa was isolated by scraping and used for Western blotting. For colitis experiments, mice were infected with adenoviral vectors on day -1 and day 1 with dextran sodium sulfate administration beginning on day 0.

Recombinant human PHB cloning and purification

The prohibitin full length cDNA was cloned into pRSETa (Invitrogen, Carlsbad, CA). This vector was transformed into *E. coli* strain BL21(DE3)pLysS (Promega, Madison, WI) and grown overnight in MagicMedia (Invitrogen). The cells were lysed with BugBuster Protein Extraction Reagent (Novagen, Gibbstown, NJ) and subsequently sonicated and centrifuged. The insoluble pellet was then solubilized in 6M urea for 1 hour and centrifuged again. Prohibitin was purified from the urea soluble fraction by elution off a HisBind Resin column following the protocol of the HisBind Purification kit (Novagen) with the following modifications: buffers were prepared with the addition of 6M urea. The column was washed with 4 volumes of binding buffer, 4 volumes of 10mM imidazole wash buffer and 4 volumes of 15mM imidazole wash buffer. Prohibitin was eluted with 3 volumes of 120 mM imidazole elution buffer and 3 volumes of 240 mM imidazole elution buffer. 5 μ l samples from each fraction were run on a 12% PAGE gel and either stained with coomassie, or transferred to nitrocellulose. Western blot of prohibitin was carried out with prohibitin antibody from Lab Vision (Fremont, CA).

Generation of PHB-loaded nanoparticles

The NPs were produced by the double-emulsion/solvent evaporation procedure described previously.¹⁷ Briefly, a primary water in oil emulsion (w/o) was prepared by mixing an organic phase (4 mL dichloromethane) containing polylactic acid (PLA) (25 g/L; M_w 75–120 kg/mol; Sigma-Aldrich, St. Louis, MO) with a homogenous internal aqueous phase (800 μ L). Recombinant human PHB (200 μ g) was mixed with polyethylenimine (PEI) (5 mM) for 10 min at room temperature allowing electrostatic interaction of PHB (negatively charged at pH = 7.2) and PEI (positively charged). BSA (50 g/L) was then added to non-bound charges of PEI. The mixture was stirred for 2 minutes with a Vortex mixer (Maxi Mix II; Thermolyne, Dubuque, IA), then sonicated (1 min, power 5, 70% active cycle, in an ice bath) using a Sonifier 450 (Branson). This primary emulsion was poured into a second aqueous phase (8 mL) (external aqueous phase) containing an amphiphilic molecule polyvinyl alcohol (PVA; 20 g/L; M_w = 13,000–23,000 g/mol; hydroxylated at 87%–89%) (Aldrich, Milwaukee, WI), which was used as the surfactant of the secondary emulsion. The water in oil in water emulsion (w/o/w) then was obtained by sonication (same conditions as those used for the primary emulsion). This double-emulsion then was transferred to an aqueous 5 g/L PVA dispersing phase (40 mL) and stirred for 5 minutes. The organic solvent was evaporated under stirring and low vacuum conditions (Rotary evaporator, Yamato RE200) and the collected solid nanospheres were resuspended in water and then centrifuged again to remove the excess PVA. This purification procedure was repeated twice. The final suspension then was freeze-dried. Nanoparticles covered with PVA and containing

fluorescent FITC-tagged PHB (molecular weight, 250,000 g/mol; Sigma-Aldrich) were prepared according to the procedure described earlier.

Treatment of mice with PHB-loaded nanoparticles

BSA- or PHB-loaded NPs were encapsulated into a polysaccharide solution composed of 7 g/L alginate and 3 g/L chitosan for delivery to the colon. For a detailed protocol refer to Laroui et al., 2010.¹⁷ NPs were added to the polysaccharide solution to obtain 5 mg of NPs per ml of solution. Using the double gavage procedure previously described (a detailed protocol is available at http://www.natureprotocols.com/2009/09/03/a_method_to_target_bioactive_c.php), 200 μ l polysaccharide solution containing NPs was gavaged first, followed by 100 μ l of the chelation solution containing 70 mmol/L of calcium chloride and 30 mmol/L sodium sulfate. A hydrogel solution encapsulated with NPs was formed by the mixture of these two solutions in the mouse stomach. For visualization of PHB-loaded NPs, mice were gavaged with FITC-tagged PHB-loaded NPs/chelation solution once per day for 4 days and sacrificed on day 5. Colon was isolated and fluorescence was assessed by confocal microscopy. For colitis experiments, mice were gavaged with BSA- or PHB-loaded NPs/chelation solution once per day starting on day -1 through day 4; DSS was administered on day 0 and mice were sacrificed on day 6. Control mice were gavaged with hydrogel without NPs/chelation solution and given water throughout the study period.

Induction of DSS Colitis

Colitis was induced in wild-type C57BL/6J male 8-week old mice were purchased from Jackson Laboratories by oral administration of dextran sodium sulfate (DSS) (molecular weight, 50,000; MP Biomedicals, Solon, OH) at 3% (wt/vol) in tap water ad libitum for 6 days (NPs experiment) or 7 days (adenovirus experiment). Age-matched male WT receiving normal tap water served as controls. Mean DSS water consumption, body weight, and development of clinical symptoms were assessed daily during the treatment period.

Endoscopic assessment of colitis

Direct visualization of DSS-induced colonic mucosal damage in vivo was performed using the Coloview (Karl Storz Veterinary Endoscopy, Tuttlingen, Germany). Mice were supplied with food and water until the endoscopy was performed. Mice were anesthetized with 1.5 to 2% isoflurane and 3 cm of the colon proximal to the anus was visualized after inflation of the colon with air. The endoscopic damage score was determined using a previously described scoring method with one modification: assessment of colon translucency (0–3 points), presence of fibrin attached to the bowel wall (0–3 points), granular aspect of the mucosa (0–3 points), morphology of the vascular pattern (0–3 points), and stool characteristic (normal to diarrhea; 0–3 points).^{18, 19} Since this scoring method did not include assessment for the presence of blood in the lumen, we added this parameter (0 points: no blood; 1 point: slight bleeding; 2 points: frank bleeding) to generate a range in total score from 0–17 points.

Clinical Activity Score

Assessment of body weight loss, stool consistency, and the presence of occult/gross blood by a guaiac test (Hemoccult Sensa; Beckman Coulter, Fullerton, CA) were determined daily for each mouse to generate a clinical activity score as previously described (20). Each parameter was scored as follows: body weight change: no change (score 0), weight loss of 1–5% (score 1), 5–10% loss (score 2), 10–20% loss (score 3), and more than 20% loss (score 4); stool character: normal (score 0), soft with well-formed pellets (score 1), soft without pellets (score 2), or diarrhea (score 4); occult blood: no blood (score 0), positive

hemocult (score 2), and gross bleeding (score 4). These scores were added to get a clinical activity score ranging from 0 to 12.

Histological assessment of colitis

Distal colon was fixed in formalin and stained with H&E. Sections were coded for blind microscopic assessment of inflammation. Histological scoring was performed on the basis of 3 parameters as previously described:²⁰ the severity of inflammation, crypt damage and ulceration. Each parameter was scored as follows: inflammation: rare inflammatory cells in the lamina propria (score 0), increased numbers of granulocytes in the lamina propria (1 point), confluence of inflammatory cells extending into the submucosa (2 points), and transmural extension of the inflammatory infiltrate (3 points); crypt damage: intact crypts (0 points), loss of the basal one-third (1 point), loss of the basal two-thirds (2 points), entire crypt loss (3 points), a change of epithelial surface with erosion (4 points), and confluent erosion (5 points); ulceration: an absence of ulcer (0 points), 1 or 2 foci of ulcerations (1 point), 3 or 4 foci of ulcerations (2 points), and confluent or extensive ulceration (3 points). These values were totaled to give a score range of 0–11 points. A minimum of 3 sections of different parts of the distal colon per animal were scored.

Western blot analysis

Total protein was isolated from colon mucosa from WT mice infected with AdPHB or AdV. The samples were separated by SDS-PAGE using Laemmli's 2X SDS sample buffer and 12% gradient polyacrylamide gels followed by electrotransfer to nitrocellulose membranes. Membranes were incubated with primary antibodies at 4°C overnight and subsequently incubated with corresponding peroxidase-conjugated secondary antibodies. Mouse monoclonal PHB antibody was obtained from Lab Vision and mouse monoclonal GFP antibody from Santa Cruz Biotechnology (Santa Cruz, CA). Membranes were washed and immunoreactive proteins were detected using Western Lightning Chemiluminescence Reagent Plus (Perkin Elmer, Boston, MA) and exposed to high performance chemiluminescence film (Denville, Metuchen, NJ). Blots were reprobred with anti- β -tubulin (Sigma-Aldrich) antibody as a loading control.

Myeloperoxidase activity

Neutrophil infiltration into the distal colon (DSS-induced colitis) was quantified by measuring myeloperoxidase (MPO) activity. Briefly, a portion of colon or cecum was homogenized in 1:20 (wt/vol) 50 mmol/L phosphate buffer (pH 6.0) containing 0.5% hexadecyltrimethyl ammonium bromide on ice by using a Polytron homogenizer. The homogenate was sonicated for 10 seconds, freeze-thawed 3 times, and centrifuged at 14,000 rpm for 15 minutes. Supernatant was added to 1 mg/mL of *o*-dianisidine hydrochloride and $5 \times 10^{-4}\%$ hydrogen peroxide, and the change in absorbance at 460 nm was measured. One unit of MPO activity was defined as the amount that degraded 1 μ mol of peroxidase per minute at 25°C.

RNA isolation and quantitative real-time PCR analysis

The proinflammatory cytokines tumor necrosis factor (TNF) α , interleukin-1 (IL-1) β , and interferon (IFN) γ were measured by real-time PCR. Total RNA was isolated from distal colon using the RNeasy kit (Qiagen, Valencia, CA) and was then reverse transcribed using the First Strand cDNA Synthesis Kit (Fermentas, Glen Burnie, MD). 50 ng of reverse-transcribed cDNA was amplified by quantitative RT-PCR using 10 μ M gene-specific primers and iQ SYBR Green Supermix (Bio-Rad, Hercules, CA) using the following PCR conditions: initial denaturation of one cycle at 95°C for 10 minutes, followed by amplification at 95°C for 30 seconds, 60°C for 30 seconds, and 72°C for 30 seconds for 35

cycles. Expression level of β -actin was used as an internal control. Raw cycle threshold values (Ct values) obtained for TNF α , IL-1 β , and IFN γ were deducted from the Ct value obtained for internal β -actin transcript levels. For graphical representation of quantitative PCR data, the $\Delta\Delta C_T$ was calculated as follows: $\Delta\Delta C_T = (Ct_{\text{target}} - Ct_{\beta\text{-actin}})_{\text{control}} - (Ct_{\text{target}} - Ct_{\beta\text{-actin}})_{\text{DSS}}$, with the final graphical data derived from $2^{-\Delta\Delta C_T}$. The following primers were utilized for quantitative RT-PCR: β -actin: 5'-TATGCCAACACAGTGCTGTCTGG-3' and 5'-TACTCCTGCTTGCTGATCCACAT-3'. TNF α sense 5'-AGGCTGCCCCGACTACGT-3', antisense 5'-GACTTTCTCCTGGTATGAGATAGCAA-3'; IL-1 β sense 5'-TCGCTCAGGGTCACAAGAAA-3', antisense 5'-CATCAGAGGCAAGGAGGAAAAC-3'; IFN γ sense 5'-CAGCAACAGCAAGGCGAAA-3', antisense 5'-CTGGACCTGTGGGTTGTTGAC-3'.

Protein carbonyl content

The oxidative damage to proteins was assessed using a protein carbonyl assay kit (Cayman Chemicals, Ann Arbor, MI). Briefly, carbonyl groups were measured based on the reaction of protein carbonyls with 2,4-dinitrophenylhydrazine, forming a Schiff base to produce the corresponding hydrazone, which is analyzed spectrophotometrically at 360 nm. Carbonyl content is normalized to total protein content.

NPs size and potential zeta measurement

Diameter (nm) and zeta potential (mV) of NPs were measured by light scattering using 90 Plus/BI-multi angle particle sizing or by light scattering after applying an electric field using a ZetaPlus Zeta Potential Analyzer (Brookhaven Instruments, Holtsville, NY). Average and standard deviation of diameter or zeta potential were calculated using 3 runs of 10 measurements each run.

Cytotoxicity test

The lactate dehydrogenase (LDH) test determines the secretion of LDH into the culture medium from dead or membrane-damaged cells. 10,000 cells were plated and exposed to 500 μ g/ml BSA- or PHB-loaded NPs or lipofectamine for 30 h. An aliquot (100 μ l) of culture media was added to 100 μ l of LDH reagent and % cytotoxicity and cell proliferation (% of total cells) were determined according to the manufacturer's protocol (Clontech, Mountain View, CA).

Cell culture

The Caco2-BBE human intestinal epithelial cell line was used as an in vitro model of polarized intestinal epithelium. All cells were grown as a confluent monolayer in Dulbecco's modified Eagle medium supplemented with 40 mg/L penicillin, 90 mg/L streptomycin, and 10% fetal calf serum. All experiments were performed on Caco2-BBE cells between passages 20 and 30. For all experiments Caco2-BBE cells were plated onto permeable supports (pore size, 0.4 μ m; Transwell-Clear polyester membranes; Costar Life Sciences, Acton, MA).

NF- κ B luciferase reporter assays

To determine whether PHB-NPs has biological activity, Caco2-BBE cells plated on permeable supports were co-transfected with 20 ng of pRL-CMV (renilla luciferase) and the pNF- κ B-Luc plasmid (Clontech Laboratories, Mountain View, CA), which contains multiple copies of the NF- κ B consensus sequence fused to a TATA-like promoter region from the herpes simplex virus thymidine kinase promoter upstream of the firefly luciferase reporter gene. The reporter gene is activated when endogenous NF- κ B proteins bind the

multiple copies of the NF- κ B sequence. 24 h after transfection, apical culture media was replaced with media containing 500 μ g/ml BSA- or PHB-loaded NPs. 48 h later, cells were serum-deprived and treated with 10 ng/ml TNF α on the basolateral side for 6 h. Luciferase activity was measured using the Dual-Luciferase Reporter Assay System (Promega) and a Luminoskan Ascent luminometer (Thermo Electron, Waltham, MA). Relative luciferase was calculated by normalizing firefly luciferase activity to Renilla luciferase activity of the pRLCMV vector.

Electrophoretic mobility shift assay (EMSA)

To determine whether PHB-NPs has biological activity, nuclear protein extracts were isolated from Caco2-BBE cells exposed to 500 μ g/ml BSA- or PHB-loaded NPs for 72 h and then treated with 10 ng/ml TNF α on the basolateral side for 30 min. Nuclear protein was assayed for DNA binding to biotin-labeled, double-stranded oligonucleotides containing the consensus NF- κ B-binding site (5'-AGTTGAGGGGACTTTCCAGGC-3') (Promega). The oligonucleotides were end-labeled using the Biotin 3' End DNA Labeling kit (Pierce, Rockford, IL) according to manufacturer's instructions. EMSAs were performed using the Lightshift Chemiluminescent EMSA kit (Pierce). Biotin-labeled oligonucleotide, 20 fmol, was incubated with 10 μ g nuclear proteins for 20 min at room temperature in binding buffer (50 mM Tris, pH 7.4, 2.5 mM EDTA, 0.25 mg/ml poly(dI/dC), 250 mM NaCl, 2.5 mM DTT, 5 mM MgCl₂, and 20% glycerol). Binding was competed by fourfold excess unlabeled NF- κ B oligonucleotides (cold). NF- κ B-binding complexes were resolved by electrophoresis using 5% TBE Criterion gels (Bio-Rad), transferred to Biodyne B Precut Modified Nylon membranes (Pierce), UV cross-linked, and visualized using the Chemiluminescent Nucleic Acid Detection System (Pierce). For NF- κ B supershift, 2 μ g p50 antibody (Millipore, Billerica, MA) was added after incubation of the 10 μ g nuclear proteins with the biotin-labeled oligonucleotides and was subsequently incubated for 30 min at room temperature.

Confocal Microscopy

Confocal microscopy was used to visualize GFP localization in 7 μ m paraffin sections from colon of mice infected with AdPHB. Confocal microscopy was also used to visualize FITC localization in Caco2-BBE cells exposed to 500 μ g/ml BSA- or FITC-tagged PHB-loaded NPs for 72 h as well as FITC localization in 7 μ m paraffin sections from colon of mice gavaged with FITC-tagged PHB-loaded NPs for 4 days. Samples were fixed in buffered 4% paraformaldehyde for 20 min, blocked in 2% bovine serum albumin and counterstained with rhodamine/phalloidin (Molecular Probes, Eugene, OR) to visualize actin and DAPI (Molecular Probes) to visualize nuclei. Samples were mounted in p-phenylenediamine/glycerol (1:1) and analyzed by confocal microscopy (Zeiss dual-laser confocal microscope).

Scattering and transmission electron microscopy of NPs

Suspensions of 1 mg/ml NPs on plots were fixed with gluteraldehyde containing 2.5% cacodylate buffer (0.1 mol/L, pH 7.0) overnight at 4°C. The samples were rinsed and dehydrated in increasing alcohol concentrations (30%, 50%, 70%, 80%, 90%, 100% vol/vol), incubated for 5 min with hexamethyldisilazane and dried under a range hood. The samples were then fixed on an aluminum support with carbon-adhesive glue and coated with gold palladium (Spotter Coater SC7640) and visualized on a scanning electron microscopy (Cambridge Instruments Stereoscan S). For transmission electron microscopy, samples were dehydrated, embedded in epoxy resin, and transverse sections were cut 70 nm thick and visualized on a transmission electron microscope (model H-7500; Hitachi, Pleasanton, CA). Caco2-BBE cells exposed to 500 μ g/ml PHB-loaded NPs for 48 hr were also processed for transmission electron microscopy as described above.

Statistical Analysis

Values are expressed as mean \pm SEM. Comparisons between PHB adenovirus or PHB-loaded NPs treatment and DSS colitis were analyzed by two-way analysis of variance to test for a significant interaction between severity of colitis and PHB overexpression. Subsequent pairwise comparisons used Bonferroni post-hoc tests to test for significant differences between two particular groups. $p < 0.05$ was considered statistically significant in all analyses.

Results

GFP is expressed in superficial colonic epithelial cells 1 and 3 days post-infection in mice administered AdPHB

Mice were infected with 2×10^9 adenoviral-vector (AdV) or adenoviral-PHB (AdPHB) plaque-forming units (PFU) in 50 μ l of phosphate-buffered saline (PBS) by intrarectal enema. Control mice were given an enema of PBS alone. Mice were sacrificed on days 1, 3 and 5 post-infection and colon was obtained for visualization of GFP expression or mucosa was isolated by scraping for total protein isolation. Using a GFP antibody, Western blotting showed PHB-GFP expression (59 kDa) in mice infected with AdPHB on days 1 and 3 post-infection in colon mucosa (Figure 1a). One day post-infection showed the highest PHB-GFP expression with less on day 3 and none on day 5 post-infection. This is likely due to loss of infected cells due to turnover of the intestinal epithelium and the nature of the adenovirus constructs being non-replicative. Similarly, the highest expression of PHB was noted 1 day post-infection, likely due to cleavage of GFP from PHB by endogenous proteases (Figure 1a). GFP expression was localized primarily in the distal colon with no expression detected in the proximal colon or ileum (data not shown). GFP expression was localized to multiple surface colonic epithelial cells in mice administered AdPHB compared to mice administered PBS (Figure 1b–e).

Exogenous AdPHB-dependent inhibition of DSS-induced colitis

Since enema delivery resulted in transient expression of GFP in the colon, mice were given an enema of PBS alone or PBS containing 2×10^9 AdV or AdPHB PFU twice during the course of the experiment; on day -1 and day 2 of dextran sodium sulfate (DSS) administration. 24h after administration of the first enema, mice were given 3.0% DSS in their drinking water for 7 days to induce colitis. Control mice were given water alone. On day 2 of DSS administration, mice were infected a second time with 2×10^9 AdV or AdPHB PFU. The DSS model of colitis shares a number of features in common with acute colitis of human IBD.²¹

Mice infected with AdV or AdPHB and given water as a control showed no overt signs of intestinal inflammation as indicated by changes in body weight throughout the study period (Figure 2a). AdV-infected mice given DSS began to lose weight on day 5 of DSS treatment and lost 5.9% of the starting body weight by day 7 of treatment. AdPHB-infected mice given DSS showed no body weight loss by day 7 of treatment and did not vary significantly from water control mice (Figure 2a).

A clinical score was assigned on the day of sacrifice (day 7 of DSS treatment), which is a well-established tool for assessing severity of disease in this animal model. Three parameters consisting of weight loss, stool consistency (diarrhea), and the presence of fecal blood are totaled to generate a clinical score. Mice infected with AdPHB exhibited a lower score for weight loss and stool consistency than mice infected with AdV, resulting in a lower total clinical score (Figure 2b).

Myeloperoxidase (MPO) activity, a marker of neutrophil activation, was measured in distal colon. There was no difference in MPO activity between AdV- or AdPHB-infected mice given water (Figure 2c). MPO activity was increased in AdV-infected mice treated with DSS compared with water controls. AdPHB-infected mice given DSS showed significantly less MPO activity compared with AdV-infected mice given DSS (Figure 2c).

Colonic expression of the pro-inflammatory cytokines TNF α , interleukin-1 beta (IL-1 β), and interferon gamma (IFN γ) were measured by quantitative real-time PCR. There was no difference in cytokine mRNA expression between AdV- or AdPHB-infected mice given water (Figure 2d). TNF α , IL-1 β , and IFN γ expression were induced to a lesser degree in AdPHB-infected mice treated with DSS compared to AdV-infected mice given DSS (Figure 2d).

Our previous study showed that villin-PHB transgenic mice, which overexpress PHB in intestinal epithelial cells, were protected from inflammation-associated oxidative stress.¹⁵ We therefore measured oxidative stress by protein carbonyl content, a marker of protein oxidation, in colonic tissue from adenovirus infected mice during DSS colitis. AdPHB-infected mice given DSS showed significantly less protein carbonyl content compared with AdV-infected mice given DSS (Figure 2e). Control mice administered an enema of PBS alone exhibited body weight changes, clinical score, MPO activity, cytokine mRNA expression and protein carbonyl content similar to AdV-infected mice (data not shown).

Mice infected with AdPHB have reduced endoscopic and histologic damage induced by DSS compared to mice administered AdV

On the day of sacrifice, inflammation was assessed macroscopically using a mouse colonoscope and an endoscopic score was calculated as described in the Methods section. Mice infected with AdV or AdPHB and given water exhibited healthy colonic mucosa (Figure 3a and b). AdV-infected mice treated with DSS showed bloody diarrhea and mucosal inflammation (Figure 3c) as compared to AdPHB-infected mice treated with DSS which showed relatively healthy mucosa (Figure 3d). No difference in endoscopic score was observed between control AdV and AdPHB infected mice given water (Figure 3m). During DSS-induced colitis, mice infected with AdV displayed significantly more severe endoscopic damage compared to mice infected with AdPHB (Figure 3m).

Acute colitis induced by DSS treatment is histopathologically characterized by infiltration of inflammatory cells into bowel wall, crypt loss, and epithelial ulceration. The most severely affected segment of bowel is the distal colon. Multiple sections of distal colon from each mouse were stained with H&E to assess the histological inflammation. Sections from mice infected with AdV or AdPHB and given water were histologically healthy (Figure 3e, f, i, j). Sections from AdV-infected mice treated with DSS exhibited severe inflammatory infiltration throughout the mucosa and submucosa, complete or partial crypt loss in some areas, and increased ulceration (Figure 3g and k). Although sections from AdPHB-infected mice treated with DSS showed increased inflammatory infiltration, crypt damage and ulceration compared to water treated mice, the severity of all three parameters was reduced compared to AdV-infected mice given DSS (Figure 3h and l). This resulted in a less severe total histological score for AdPHB-infected mice compared to AdV-infected mice during DSS treatment (Figure 3n). The total histological score correlated with the clinical indicators of disease including macroscopic findings by mouse colonoscope, clinical score, and MPO activity.

Characterization of PHB-loaded nanoparticles (NPs)

In order to assess the therapeutic potential of prohibitin, we used a nanoparticle-based strategy to deliver prohibitin directly to the colon. We recently reported synthesis of poly(lactic acid)/polyvinyl alcohol based NPs that was designed for colonic delivery.¹⁷ These NPs were designed to release the contents at pH 6.0, thus escaping degradation from acidic pH and digestive enzymes. NPs loaded with 1 mg/ml PHB were generated as described previously.²² Briefly, PHB was complexed to polyethyleneimine (PEI) and then to bovine serum albumin (BSA). This was then surrounded by the biodegradable polymer poly(lactic acid) (PLA) in a water/oil emulsion to form the core of the NPs. The core of the NPs is surrounded by a shell composed of polyvinyl alcohol (PVA) in a second water/oil/water emulsion. Zeta potential (surface charge) and size, two important characteristics of NPs that influence the efficiency by which NPs interact with cells, were determined. There was no difference between the zeta potential of BSA-loaded NPs (−4.65 mV) compared to PHB-loaded NPs (−4.73 mV), indicating the same surface charge and an unlikely potential to form aggregates (since electrostatic repulsion occurs between negatively charged NPs). Diameters of NPs were measured by light scattering theory and indicated no significant difference in size between PHB-loaded NPs (439.4 nm; Figure 4a) and BSA-loaded NPs (444.5 nm; data not shown). Scanning electron microscopy of a suspension of PHB-loaded NPs confirmed the size measured by light scattering (Figure 4b). Transmission electron microscopy (TEM) of a suspension of PHB-loaded NPs (Figure 4c) also confirmed the diameter and also allowed visualization of the electron dense hydrophobic NPs core (black) composed of PLA and the hydrophilic shell composed of PVA (white). A lactate dehydrogenase test assessed Caco2-BBE cell cytotoxicity when exposed to PHB-loaded NPs for 30 hr. Cells exposed to PHB-loaded NPs showed no cytotoxicity compared to cells exposed to BSA-loaded NPs or cells left untreated (Figure 4d). Interestingly, cells exposed to Lipofectamine 2000 transfection reagent showed a decrease in cell integrity compared to untreated cells and NPs-exposed cells (Figure 4d).

PHB-loaded NPs reduced TNF α -induced NF- κ B activation in Caco2-BBE cells

Since Caco2-BBE cells showed no cytotoxicity when exposed to PHB-loaded NPs, we next determined whether PHB-loaded NPs are taken up by Caco2-BBE cells in culture. Confluent monolayers of cells were exposed to FITC-tagged PHB-loaded NPs for 30 hr and visualized by confocal microscopy and TEM. FITC expression is detected in the cytosol of multiple Caco2-BBE cells after exposure to FITC-tagged PHB-loaded NPs compared to untreated cells (Figure 5a). TEM showed multiple PHB-loaded NPs in the cytosol of a Caco2-BBE cell (Figure 5b). These results suggest that cultured intestinal epithelial cells take up PHB-loaded NPs within 30 hr of exposure.

In order to ascertain whether PHB-loaded NPs are biologically active within the cell, we determined whether cells exposed to PHB-loaded NPs are protected against the pro-inflammatory effects of TNF α as we previously reported using DNA transfection of PHB.¹⁴ We previously reported that overexpression of PHB using DNA transfection reduces the potency that TNF α induces NF- κ B activation in Caco2-BBE cells.¹⁴ NF- κ B activation was first measured using a luciferase reporter construct. Caco2-BBE cells were transfected with the pNF- κ B-Luc plasmid which contains multiple copies of the NF- κ B consensus sequence fused to a region of the Herpes simplex virus thymidine kinase promoter upstream of the firefly luciferase reporter gene. Therefore, expression of firefly luciferase is a measure of NF- κ B promoter activation. 24 hr after transfection with the pNF- κ B-Luc plasmid cells were exposed to BSA- or PHB-loaded NPs for 72 hr, followed by stimulation with TNF α for 6 hr. TNF α increased luciferase activity approximately 7.3-fold in cells exposed to BSA-loaded NPs and approximately 4.3-fold in cells exposed to PHB-loaded NPs compared to untreated cells; PHB overexpression caused a 42% reduction in TNF α -stimulated NF- κ B luciferase

activity (Figure 5c) which is similar to the response reported with PHB overexpression using DNA transfection.¹⁴

We also performed electrophoretic mobility shift assay (EMSA) to assess TNF α -induced transcription factor binding to consensus NF- κ B binding site oligonucleotides as a second measure of NF- κ B activation. Caco2-BBE cells were exposed to BSA- or PHB-loaded NPs for 72 hr, followed by stimulation with TNF α for 30 min. Nuclear protein extracts show increased binding to the consensus NF- κ B site after TNF α treatment in cells exposed to BSA- or PHB-loaded NPs (Figure 5d). In PHB-loaded NPs exposed cells however, nuclear protein extracts show a less robust increase in binding to the NF- κ B site after TNF α treatment compared to BSA-loaded NPs exposed cells. These results suggest that TNF α -stimulated transcription factor binding to the consensus NF- κ B site is reduced by PHB overexpression delivered by NPs. Binding is competed by unlabeled NF- κ B oligonucleotides (cold) and shifted by the addition of a p50 antibody (Figure 5d). Collectively, these results suggest that PHB delivered to cultured intestinal epithelial cells by NPs is biologically active and generates responses similar to previously published data.

Mice treated with PHB-loaded NPs exhibited less severe DSS-induced colitis

BSA- or PHB-loaded NPs were encapsulated into a polysaccharide solution composed of 7 g/L alginate and 3 g/L chitosan for delivery to the colon as previously described.¹⁷ NPs were added to the polysaccharide solution to obtain 5 mg of NPs per ml hydrogel. Using the double gavage procedure previously described,¹⁷ 200 μ l polysaccharides solution containing NPs was gavaged first, followed by 100 μ l of the chelation solution containing 70 mmol/L of calcium chloride and 30 mmol/L sodium sulfate. A hydrogel encapsulated with NPs was formed directly in the mouse stomach when the ionic solution mixed with the polysaccharide solution. For visualization of PHB-loaded NPs, mice were gavaged with FITC-tagged PHB-loaded NPs/chelation solution once per day for 4 days and sacrificed on day 5. Colon was isolated and fluorescence was assessed by confocal microscopy. FITC expression was localized to the colonic surface epithelium throughout the colon. Figure 6a shows FITC expression in the epithelium of the distal colon.

Mice were gavaged with BSA- or PHB-loaded NPs/chelation solution once per day starting on day -1 through day 4; DSS was administered on day 0 and mice were sacrificed on day 6. Control mice were gavaged with hydrogel without NPs/chelation solution and given water throughout the study period. Control mice gavaged with hydrogel alone and given water showed no overt signs of intestinal inflammation as indicated by changes in body weight throughout the study period (Figure 6b). Mice treated with BSA-loaded NPs and given DSS began to lose weight on day 4 of DSS treatment and lost 5.6% of the starting body weight by day 6 of treatment. Mice treated with PHB-loaded NPs given DSS showed significantly less weight loss by day 6 of treatment (Figure 6b). Similarly, mice treated with PHB-loaded NPs exhibited a lower total clinical score (Figure 6c), less MPO activity (Figure 6d), less colonic expression of the pro-inflammatory cytokines TNF α , IL-1 β , and IFN γ (Figure 6e), and colonic protein carbonyl content (Figure 6f) than mice treated with BSA-loaded NPs.

Mice treated with PHB-loaded NPs have reduced endoscopic and histologic damage induced by DSS

Inflammation was assessed macroscopically using a mouse colonoscope and histologically using sections of distal colon. Control mice gavaged with hydrogel and given water displayed healthy colonic mucosa (Figure 7a) and normal histology (Figure 7d and g). Mice treated with BSA-loaded NPs and given DSS showed mucosal erythema, the presence of blood and less visible vasculature by colonoscope (Figure 7b) and increased histological damage including inflammatory infiltration throughout the mucosa and submucosa and

complete or partial crypt loss in some areas (Figure 7e and h). Mice treated with PHB-loaded NPs and given DSS displayed less endoscopic inflammation including less severe erythema and more visible vasculature (Figure 7c) and less severe inflammatory infiltration and crypt damage compared to BSA-loaded NPs treated mice (Figure 7f and i).

Discussion

Current therapies for IBD include non-specific immunosuppressive agents that are associated with systemic side effects and targeted therapies (such as anti-TNF molecules) that are effective but need systemic administration and are limited by life threatening systemic side effects. Clearly, there is an unmet and urgent need for targeted therapies as well as means to deliver the therapeutic agent to the site of inflammation. In this manuscript, we have utilized NPs to deliver PHB, a novel therapeutic target recently shown by us to be an effective anti-inflammatory molecule in experimental colitis, to the colon. Genetic restoration of intestinal epithelial PHB levels during experimental colitis using villin-PHB transgenic mice reduced the severity of disease through sustained epithelial anti-oxidant expression and reduced NF- κ B activation, suggesting that PHB has both anti-oxidant and anti-inflammatory properties. In this study, we utilized two methods to overexpress PHB in colonic epithelial cells which show decreased expression of PHB during active inflammation. First as a proof-of-principle to demonstrate the therapeutic efficacy of PHB, we utilized adenovirus-directed administration by enema. Second, we used NPs based colonic delivery of biologically active PHB to demonstrate therapeutic use for human IBD. Both methods of delivery resulted in increased levels of PHB in the surface epithelial cells of the colon and reduced severity of dextran sodium sulfate-induced colitis in mice as measured by body weight loss, clinical score, myeloperoxidase activity, pro-inflammatory cytokine expression, histological score and protein carbonyl content (oxidative stress).

Multiple studies have utilized NPs delivery of small peptides,¹⁷ siRNA,^{22–25} vaccines,²⁶ or low molecular weight drugs.²⁷ This is the first study to show oral delivery of a biologically active protein by NPs encapsulated in hydrogel to the colon. Other studies have utilized intravenous delivery of NPs loaded with a protein of interest, but this method results in non-specific uptake to the liver and bloodstream.²⁸ In contrast, our study using oral delivery by gavage directly targets the GI tract, specifically the colon due to the pH- and time-dependent collapse of the hydrogel encapsulating the NPs.¹⁷ Our method generates optimal therapeutic delivery to the site of inflammation during colitis. PHB is a water soluble and relatively small protein (32 kDa) making it a feasible candidate to load into NPs. We show here that PHB-loaded NPs reduced the activation of NF- κ B by TNF α in Caco2-BBE cells, corroborating our previous results using DNA transfection studies and genetic overexpression in villin-PHB transgenic mice.¹⁴ Given the well-established role of epithelial NF- κ B activation in the pathogenesis of colitis, therapeutic restoration of PHB in the colonic epithelium may represent a novel target in inflammatory bowel disease.

Acknowledgments

This work was supported by National Institutes of Health grants: RO1-DK06411 (S.V.S.), RO1-DK061941 (D.M.), K01-DK085222 (A.L.T.), R01-HD057235 (W.E.T), research center grant (R24-DK064399), and the Broad Foundation grant IBD-0226R (S.V.S).

Abbreviations

DSS	dextran sodium sulfate
IBD	inflammatory bowel disease

NPs	poly (lactic acid) nanoparticle
PHB	prohibitin

References

1. Danese S, Fiocchi C. Etiopathogenesis of inflammatory bowel diseases. *World J Gastroenterol.* 2006; 12:4807–4812. [PubMed: 16937461]
2. Ma TY, Iwamoto GK, Hoa NT, et al. TNF-alpha-induced increase in intestinal epithelial tight junction permeability requires NF-kappa B activation. *Am J Physiol Gastrointest Liver Physiol.* 2004; 286:G367–G376. [PubMed: 14766535]
3. Ali S, Mann DA. Signal transduction via the NF-kappaB pathway: a targeted treatment modality for infection, inflammation and repair. *Cell Biochem Funct.* 2004; 22:67–79. [PubMed: 15027095]
4. Steinbrecher KA, Harmel-Laws E, Sitcheran R, et al. Loss of epithelial RelA results in deregulated intestinal proliferative/apoptotic homeostasis and susceptibility to inflammation. *J Immunol.* 2008; 180:2588–2599. [PubMed: 18250470]
5. Artal-Sanz M, Tsang WY, Willems EM, et al. The mitochondrial prohibitin complex is essential for embryonic viability and germline function in *Caenorhabditis elegans*. *J Biol Chem.* 2003; 278:32091–32099. [PubMed: 12794069]
6. Nijtmans LG, de Jong L, Artal Sanz M, et al. Prohibitins act as a membrane-bound chaperone for the stabilization of mitochondrial proteins. *Embo J.* 2000; 19:2444–2451. [PubMed: 10835343]
7. Dell'Orco RT, McClung JK, Jupe ER, et al. Prohibitin and the senescent phenotype. *Exp Gerontol.* 1996; 31:245–252. [PubMed: 8706794]
8. Jupe ER, Liu XT, Kiehlbauch JL, et al. Prohibitin antiproliferative activity and lack of heterozygosity in immortalized cell lines. *Exp Cell Res.* 1995; 218:577–580. [PubMed: 7796893]
9. Joshi B, Rastogi S, Morris M, et al. Differential regulation of human YY1 and caspase 7 promoters by prohibitin through E2F1 and p53 binding sites. *Biochem J.* 2007; 401:155–166. [PubMed: 16918502]
10. Wang S, Fusaro G, Padmanabhan J, et al. Prohibitin co-localizes with Rb in the nucleus and recruits N-CoR and HDAC1 for transcriptional repression. *Oncogene.* 2002; 21:388–396.
11. Wang S, Nath N, Adlam M, et al. Prohibitin, a potential tumor suppressor, interacts with RB and regulates E2F function. *Oncogene.* 1999; 18:3501–3510. [PubMed: 10376528]
12. Hsieh SY, Shih TC, Yeh CY, et al. Comparative proteomic studies on the pathogenesis of human ulcerative colitis. *Proteomics.* 2006; 6:5322–5331. [PubMed: 16947118]
13. Theiss AL, Idell RD, Srinivasan S, et al. Prohibitin protects against oxidative stress in intestinal epithelial cells. *Faseb J.* 2007; 21:197–206. [PubMed: 17135366]
14. Theiss AL, Jenkins AK, Okoro NI, et al. Prohibitin inhibits tumor necrosis factor alpha-induced nuclear factor-kappa B nuclear translocation via the novel mechanism of decreasing importin alpha3 expression. *Mol Biol Cell.* 2009; 20:4412–4423. [PubMed: 19710421]
15. Theiss AL, Vijay-Kumar M, Obertone TS, et al. Prohibitin is a novel regulator of antioxidant response that attenuates colonic inflammation in mice. *Gastroenterology.* 2009; 137:199–208. [PubMed: 19327358]
16. Chowdhury I, Xu W, Stiles JK, et al. Apoptosis of rat granulosa cells after staurosporine and serum withdrawal is suppressed by adenovirus-directed overexpression of prohibitin. *Endocrinology.* 2007; 48:206–217. [PubMed: 17038561]
17. Laroui H, Dalmaso G, Nguyen HT, et al. Drug-Loaded Nanoparticles Targeted to the Colon With Polysaccharide Hydrogel Reduce Colitis in a Mouse Model. *Gastroenterology.* 2010; 138:843–853. [PubMed: 19909746]
18. Hu S, Zhu X, Triggs JR, et al. Inflammation-induced, 3'UTR-dependent translational inhibition of Hsp70 mRNA impairs intestinal homeostasis. *Am J Physiol Gastrointest Liver Physiol.* 2009; 296:G1003–G1011. [PubMed: 19299581]

19. Vetrano S, Rescigno M, Cera MR, et al. Unique role of junctional adhesion molecule-a in maintaining mucosal homeostasis in inflammatory bowel disease. *Gastroenterology*. 2008; 135:173–184. [PubMed: 18514073]
20. Cooper HS, Murthy SN, Shah RS, et al. Clinicopathologic study of dextran sulfate sodium experimental murine colitis. *Lab Invest*. 1993; 69:238–249. [PubMed: 8350599]
21. Pizarro TT, Arseneau KO, Bamias G, et al. Mouse models for the study of Crohn's disease. *Trends Mol Med*. 2003; 9:218–222. [PubMed: 12763527]
22. Farokhzad OC, Jon S, Khademhosseini A, et al. Nanoparticle-aptamer bioconjugates: a new approach for targeting prostate cancer cells. *Cancer Res*. 2004; 4:7668–7672. [PubMed: 15520166]
23. Fattal E, Vauthier C, Aynie I, et al. Biodegradable polyalkylcyanoacrylate nanoparticles for the delivery of oligonucleotides. *J Control Release*. 1998; 53:137–143. [PubMed: 9741921]
24. Schiffelers RM, Ansari A, Xu J, et al. Cancer siRNA therapy by tumor selective delivery with ligand-targeted sterically stabilized nanoparticle. *Nucleic Acids Res*. 2004; 32:e149. [PubMed: 15520458]
25. Toub N, Bertrand JR, Tamaddon A, et al. Efficacy of siRNA nanocapsules targeted against the EWS-Fli1 oncogene in Ewing sarcoma. *Pharm Res*. 2006; 23:892–900. [PubMed: 16715379]
26. Garg NK, Mangal S, Khambete H, et al. Mucosal Delivery of Vaccines: Role of Mucoadhesive/ Biodegradable Polymers. *Recent Pat Drug Deliv Formul*. 2010; 4:114–128. [PubMed: 20380624]
27. Park JH, Saravanakumar G, Kim K, et al. Targeted delivery of low molecular drugs using chitosan and its derivatives. *Adv Drug Deliv Rev*. 62:28–41. [PubMed: 19874862]
28. Krishna AD, Mandraju RK, Kishore G, et al. An efficient targeted drug delivery through apotransferrin loaded nanoparticles. *PLoS One*. 2009; 4:e7240. [PubMed: 19806207]

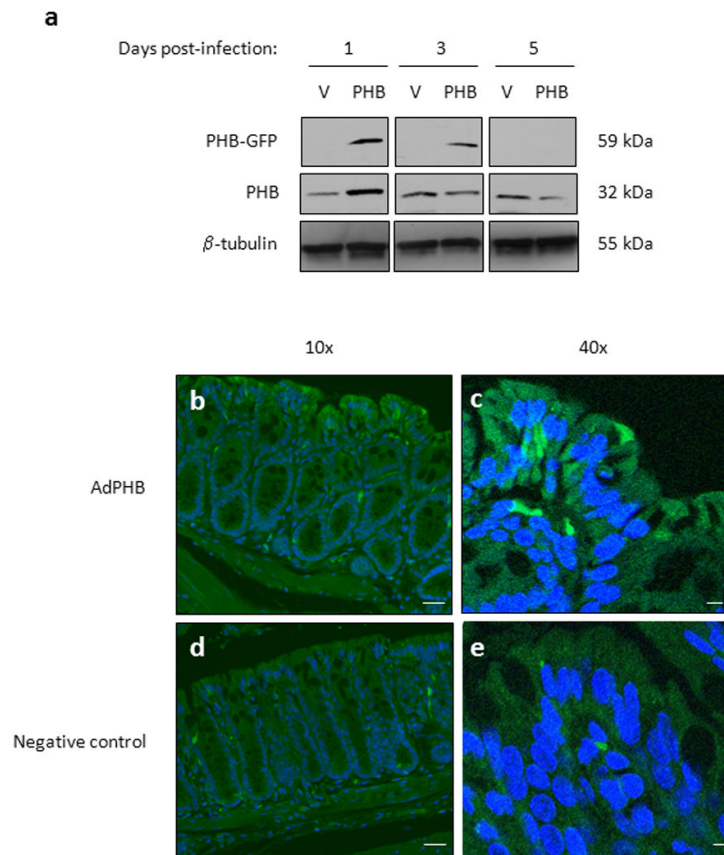


Figure 1. GFP is transiently expressed in surface colonic epithelial cells 1 and 3 days post-infection in mice administered AdPHB

Mice were administered pAdTrack-CMV-PHB1-GFP (AdPHB) or pAdTrack-CMV-GFP (AdV) by enema. (A) Western blots showing GFP, PHB, and β -tubulin (loading control) expression from total protein isolated from colon mucosa collected day 1, 3 or 5 post-infection. (B–E) To show AdPHB localization, GFP fluorescence was visualized using fluorescent microscopy (B and D) and confocal microscopy (C and E) in colon tissue isolate 1 day post-infection. GFP expression (green) was increased in surface colonic epithelial cells in mice administered AdPHB (A–B) compared to mice administered PBS (C–D). Nuclei were stained with DAPI (blue). Bar = 20 μ m in (B) and (D). Bar = 5 μ m in (C) and (E).

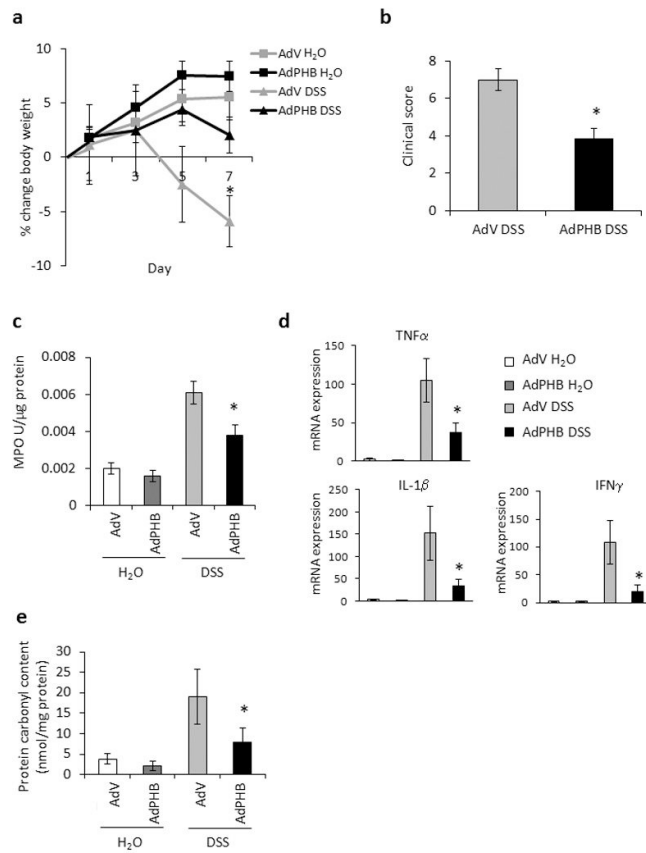


Figure 2. Exogenous AdPHB-dependent inhibition of DSS-induced colitis

(A) Percent change in body weight during DSS colitis. * $P < 0.05$ vs. all other treatment groups. (B) Changes in clinical score. * $P < 0.05$ vs. AdV. (C) Colonic myeloperoxidase activity. * $P < 0.05$ vs. AdV. (D) Quantitative real-time PCR was used to quantify mRNA levels of the cytokines tumor necrosis factor α , interleukin-1 β , and interferon γ . Values represent means \pm SEM of 2 determinations per animal. * $P < 0.05$ vs. AdV. (E) Protein carbonyl content. * $P < 0.05$ vs. AdV. $n = 5$ animals per treatment.

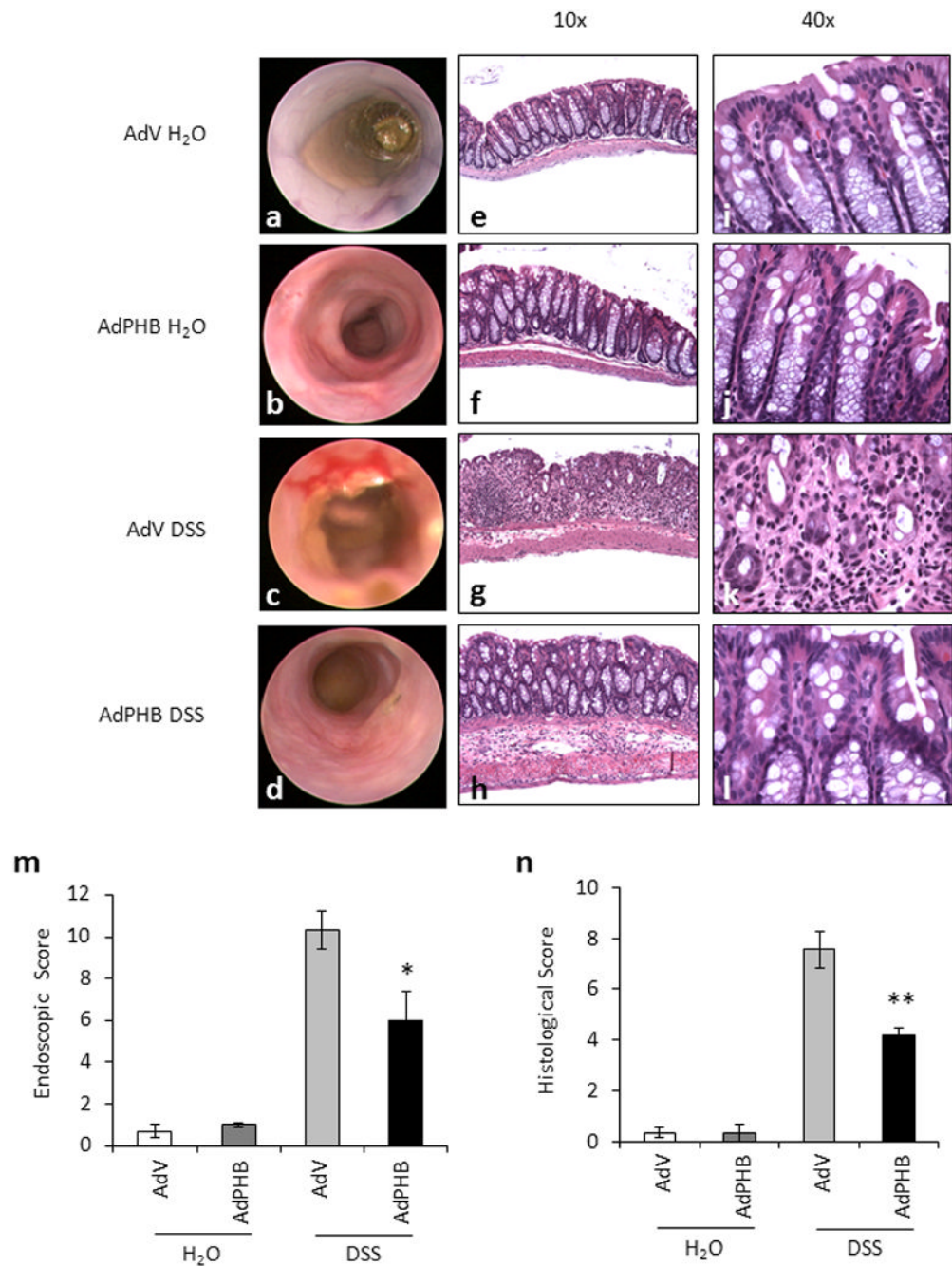


Figure 3. Mice infected with AdPHB have reduced endoscopic and histologic damage induced by DSS compared to mice administered AdV

(A–D) Macroscopic inflammation was assessed using a mouse colonoscope. Photos were obtained on the day of sacrifice and an endoscopic score was calculated. (E–L) Representative photomicrographs of paraffin-embedded H&E-stained sections of distal colon. Original magnification 10× (E–H) and 40× (I–L). (M) Endoscopic score was derived as described in the Methods section. * $P < 0.05$ vs. AdV; $n = 4$ animals per treatment. (N) Histologic score of severity of inflammatory infiltrate, extent of crypt damage and ulceration used to generate a total histological score. ** $P < 0.01$ vs. AdV; $n = 5$ animals per treatment.

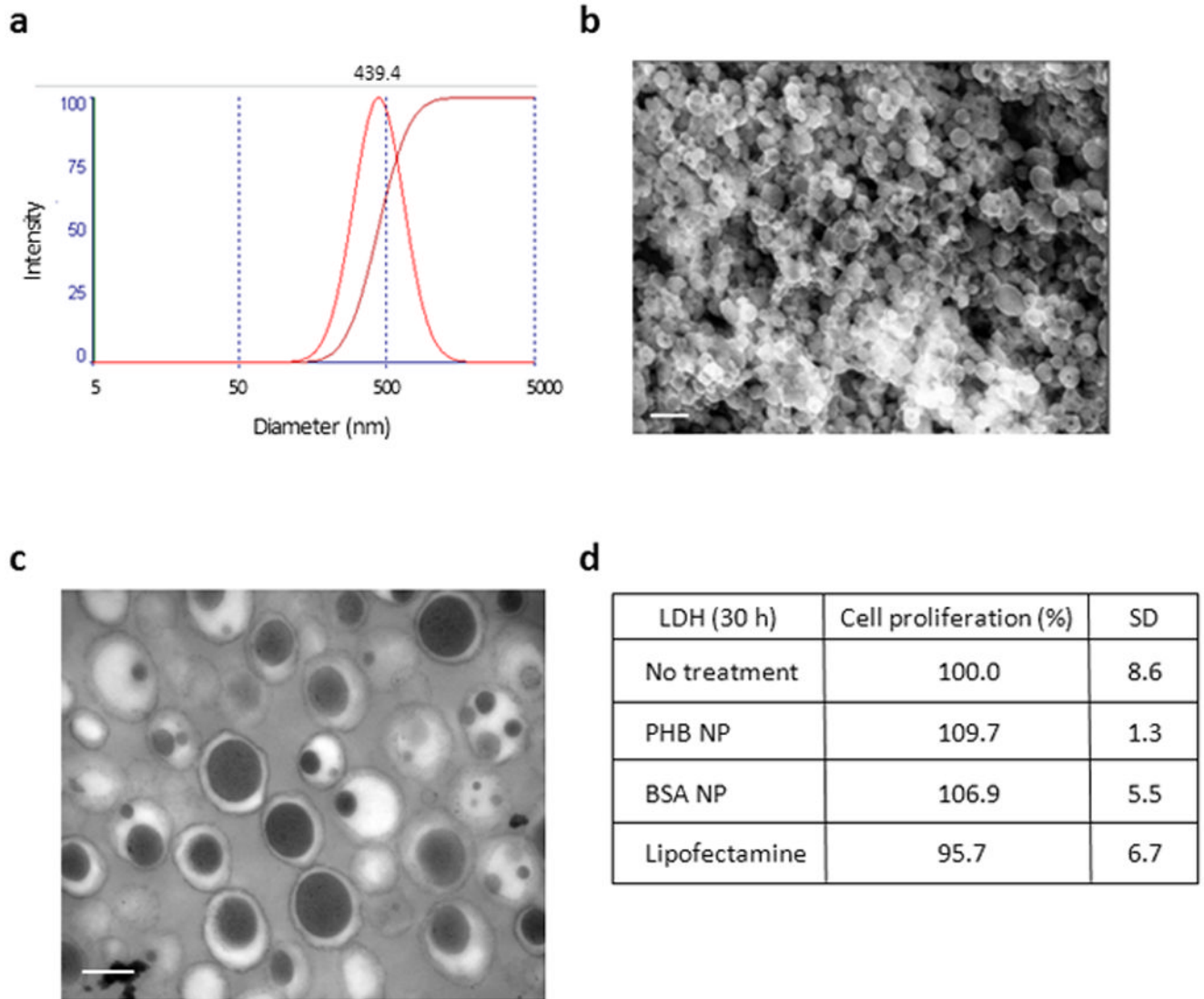


Figure 4. Characterization of PHB-loaded nanoparticles (NPs)

(A) Size distribution of PHB-loaded NPs measured by light scattering. PHB-loaded NPs are 439.4 nm in diameter. (B) Scanning electron microscopy (SEM) picture of a suspension of NPs loaded with 1 mg/ml PHB. Bar = 667 nm. (C) Transmission electron microscopy (TEM) picture of a suspension of NPs loaded with 1 mg/ml PHB. Bar = 0.2 μ m. (D) Cytotoxicity as measured by LDH test of a 1 mg/ml suspension of PHB-loaded NPs on Caco2-BBE cells for 30 hr and compared to BSA-loaded NPs and lipofectamine transfection as controls.

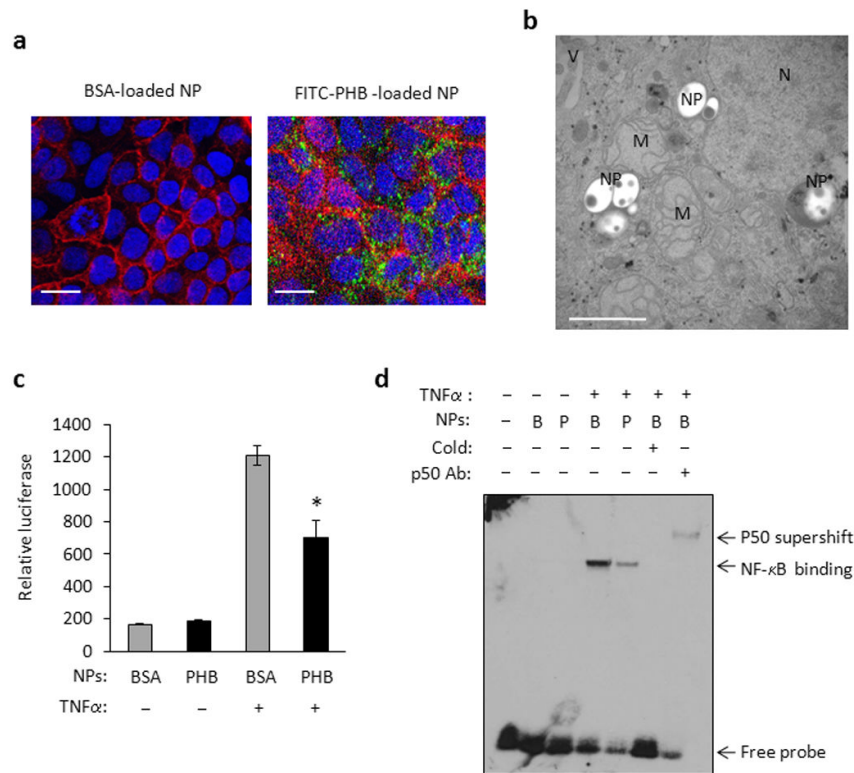


Figure 5. PHB-loaded NPs reduced TNF α -induced NF- κ B activation in Caco2-BBE cells
 (A) Confocal microscopy photograph of FITC-tagged PHB-loaded NPs (green) in polarized Caco2-BBE cell monolayers. Sections were counterstained with rhodamine/phalloidin and DAPI to visualize actin (red) and nuclei (blue), respectively. Untreated Caco2-BBE cells were used as a negative control. Bar = 20 μ m. (B) TEM picture of Caco2-BBE cell exposed to 500 μ g/ml PHB-loaded NPs for 48 hr. NPs are located in the cytosol of the cell. M, mitochondrion; N, nucleus; NPs, nanoparticle; V, villus. Bar = 1 μ m. (C) Relative luciferase activity of Caco2-BBE cells transfected with the pNF- κ B-Luc plasmid and exposed to BSA- (B) or PHB-loaded NPs for 72 hr. Cells were then treated with 10 ng/ml TNF α for 6 h. *P = 0.05 vs. vector; n = 3 per treatment. (D) EMSA showing binding of 10 μ g nuclear proteins isolated from Caco2-BBE cells exposed to BSA- (B) or PHB-loaded (P) NPs for 72 hr and treated with 10 ng/ml TNF α for 30 min. Binding is to a consensus NF- κ B site and is competed by unlabeled NF- κ B oligonucleotides (cold). The addition of a p50 antibody caused a supershift.

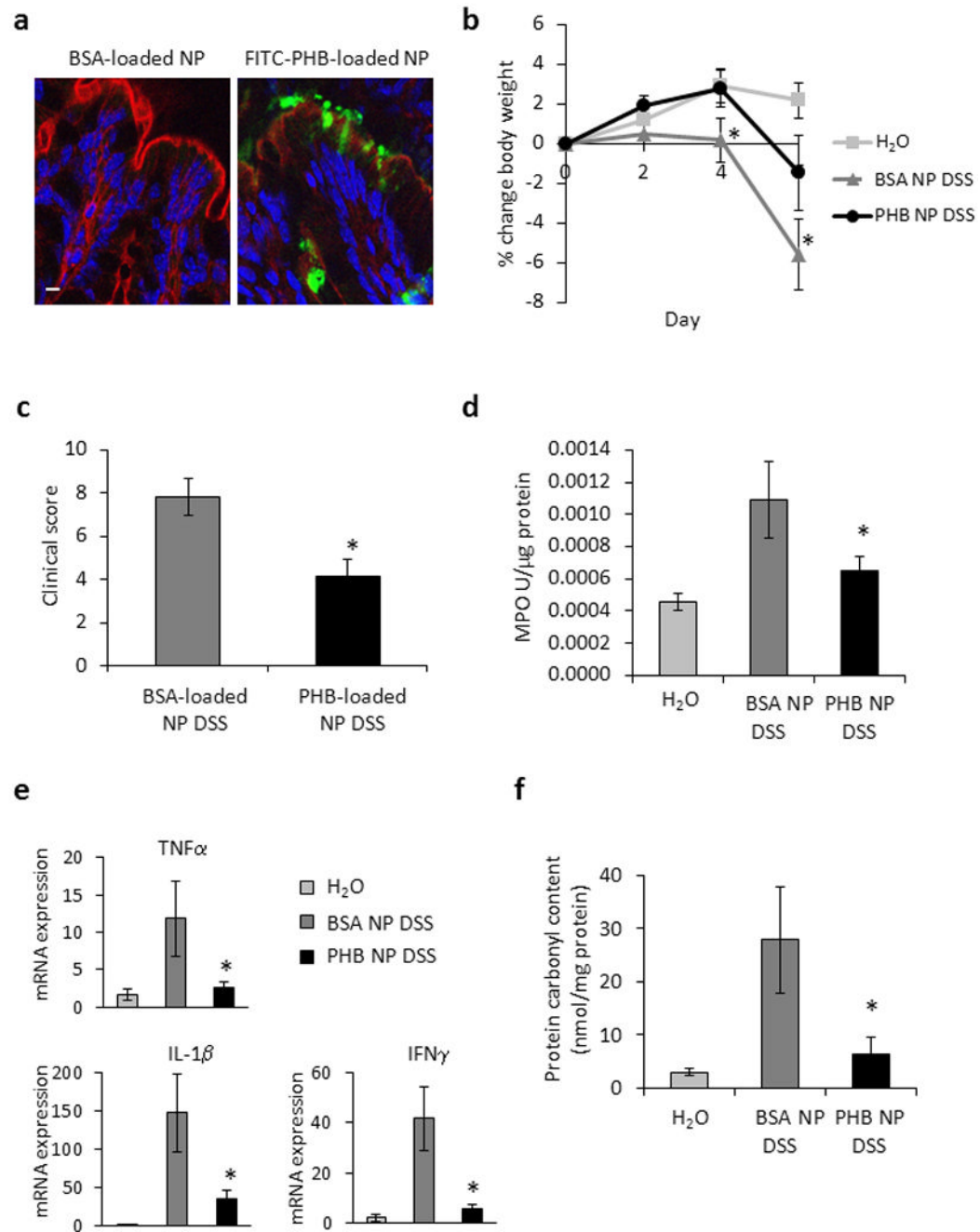


Figure 6. Mice treated with PHB-loaded NPs exhibited less severe DSS-induced colitis
 (A) FITC-PHB delivered by NPs is expressed in surface colonic epithelial cells. Colon was isolated and fluorescence was assessed by confocal microscopy. Bar = 5 μ m. (B) Percent change in body weight during DSS colitis. * $P < 0.05$ vs. all other treatment groups. (C) Changes in clinical score. * $P < 0.05$ vs. Adv. (D) Colonic myeloperoxidase activity. * $P < 0.05$ vs. Adv. (E) Quantitative real-time PCR was used to quantify mRNA levels of the cytokines tumor necrosis factor α , interleukin-1 β , and interferon γ . Values represent means \pm SEM of 2 determinations per animal. * $P < 0.05$ vs. Adv. (F) Protein carbonyl content. * $P < 0.05$ vs. Adv. $n \geq 7$ animals per treatment.

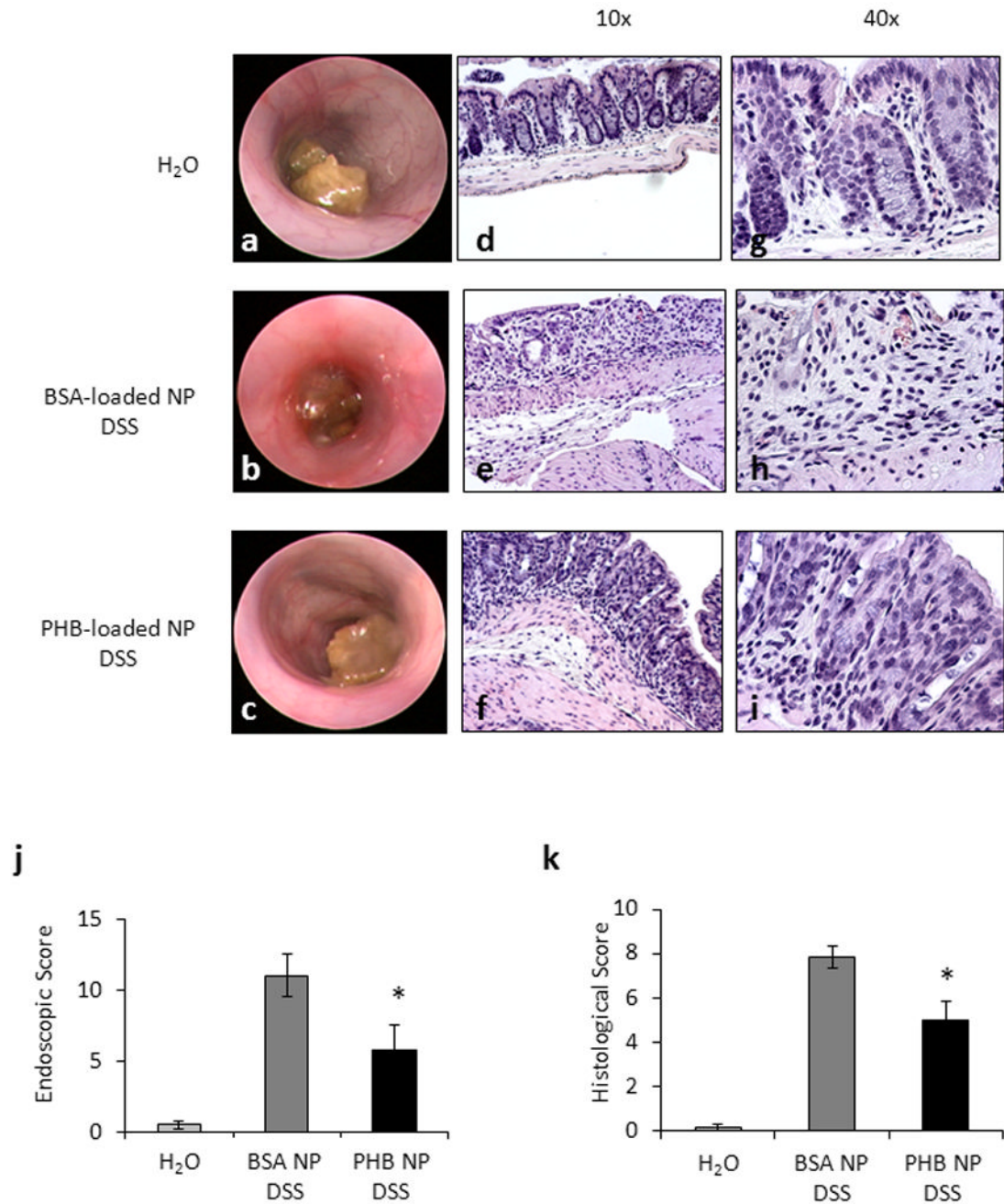


Figure 7. Mice treated with PHB-loaded NPs have reduced endoscopic and histologic damage induced by DSS

(A–C) Macroscopic inflammation was assessed using a mouse colonoscope. Photos were obtained on the day of sacrifice and an endoscopic score was calculated. (D–I) Representative photomicrographs of paraffin-embedded H&E-stained sections of distal colon. Original magnification 10× (D–F) and 40× (G–I). (J) Endoscopic score. * $P < 0.05$ vs. BSA-loaded NPs DSS; $n = 4$ animals per treatment. (N) Histologic score of severity of inflammatory infiltrate, extent of crypt damage and ulceration used to generate a total histological score. * $P < 0.05$ vs. BSA-loaded NPs DSS; $n \geq 7$ animals per treatment.